BIOCHEMISTRY

 Volume 44, Number 31 August 9, 2005

Accelerated Publications

A Definitive Mechanism for Chorismate Mutase†

Xiaodong Zhang, Xiaohua Zhang, and Thomas C. Bruice*

Department of Chemistry and Biochemistry, University of California, Santa Barbara, California 93106

Received May 12, 2005; Revised Manuscript Received June 18, 2005

ABSTRACT: In previous research presentations, we have described the important features of the chorismate → prephenate reaction using molecular dynamics (MD) and thermodynamic integration studies. This investigation of the reaction in *Escherichia coli* and water involves QM/MM procedures (SCCDFTB/MM two-dimensional reaction coordinates to identify transition state structures in the water, enzyme, and gas phase followed by B3LYP/6-31+G* single-point computations which allow the determination of activation energies in water and in the *E. coli* enzyme). Computed activation energies of 11.3 kcal/mol in enzyme and 20.3 kcal/mol in water may be compared to the experimental values of 12.7 and 20.7 kcal/mol, respectively. The transition state structures in the gas phase, water, and enzyme are much the same. The transition states are characteristic of a concerted pericyclic rearrangement. The very small differences in the partial charges of O13 in NAC and TS support only a small preferential (10%) electrostatic stabilization of TS. The free energy of NAC formation in water exceeds that in enzyme by 8.5 kcal/mol, and it is this favored formation of NAC that provides the major kinetic advantage to the enzymatic reaction. These findings compare most favorably with those previous observations of this laboratory employing molecular dynamics and thermodynamic integrations. A definitive mechanism for the chorismate mutase enzymes is provided.

We (*1*) have pointed out that the contributions of ground state conformations and transition state stabilization to the efficiency of enzyme catalysis are easiest to recognize with one-substrate enzymes involving the intramolecular rearrangement of substrate to product without formation of an enzyme−substrate covalent intermediate (*2, 3*). The Claisen rearrangement of chorismate to prephenate by chorismate mutase is the most studied example (Figure 1). For a reaction to take place, reacting atoms must come together to van der Waals separation and at angles resembling that in the transition state (TS).[1] Such near-attack conformations (NACs) are the doors through which the ground state must pass to become the TS (*1, 4*). The reaction free energy is then the sum of the standard free energy for NAC formation plus the free energy for the conversion of the NAC to the TS (eq 1).

$$\Delta G^{*} = \Delta G^{\circ}_{\mathrm{NAC}} + \Delta G_{\mathrm{TS}} \qquad (1)$$

A structure of the NAC for the Claisen reaction is provided in Figure 1. S. Hur in this laboratory (*1, 5*−*7*) has carried out detailed molecular dynamics (MD) and thermodynamic integration investigations of this reaction in chorismate mutases [*Escherichia coli* (*1, 4, 8, 9*) and *Bacillus subtilis* (*10*)], mutants of each enzyme, a catalytic antibody, and water. A plot of the free energies for NAC formation ($\Delta G^{\circ}_{\mathrm{NAC}}$)

† Supported by National Institutes of Health Grant 5R37DK9174-41.

* To whom correspondence should be addressed. Telephone: (805) 893-2044. Fax: (805) 893-2229. E-mail: tcbruice@chem.ucsb.edu.

[1] Abbreviations: NAC, near-attack conformer; QM/MM, quantum mechanics and molecular mechanics; SCCDFTB, self-consistent charge density functional tight binding; MD, molecular dynamics; CM, chorismate mutase; TS, transition state.

10.1021/bi050886p CCC: $30.25
Published on Web 07/12/2005

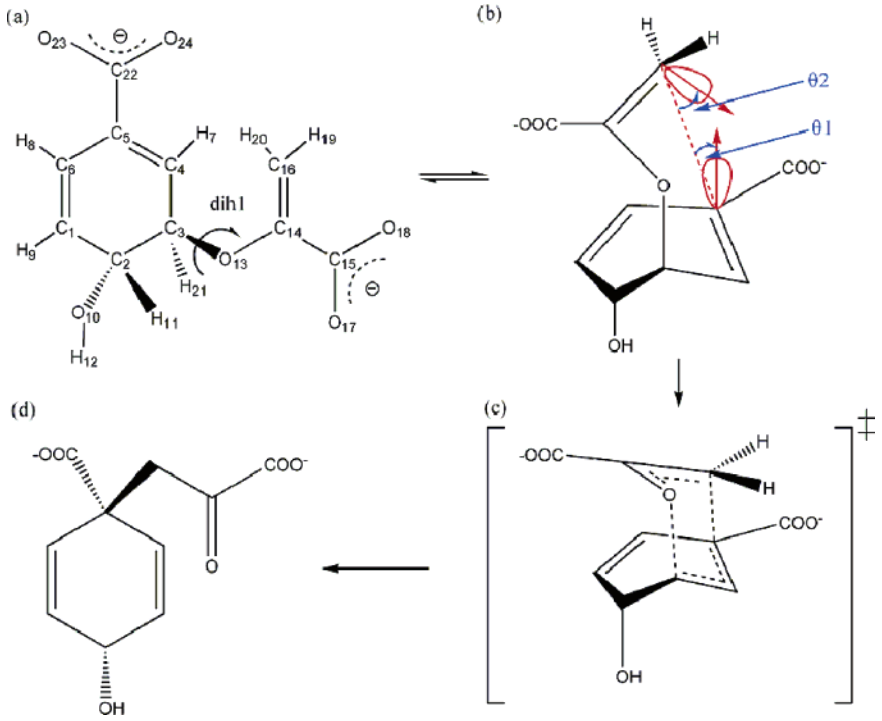

FIGURE 1: (a) Structure of chorismate. dih1 is defined as the C4−C3−O13−C14 dihedral angle. (b) Definition of NAC. θ_1 is the angle of C16 approaching the C5 π-orbital. θ_2 is the C16 π-orbital direction relative to the C5 atom. In the TS, $\theta_1 = 8.2°$ and $\theta_2 = 18.6°$. For NACs, we allow ±20° deviations ($\Delta\theta_1 \leq 20°$ and $\Delta\theta_2 \leq 20°$). The distance from C5 to C16 is ≤3.7 Å. (c) Transition state. (d) Prephenate.

versus the experimental free energies of reactions (ΔG^*) provided a linear plot [slope of 1.1, correlation coefficient of 0.97 (*7*)]. The only explanation allowed is that the free energy conversion of the NAC to the TS (ΔG_{TS}) is virtually a constant so that the enzyme creates the reactive NAC ground state and the reaction occurs almost spontaneously. The rates of reactions in the six systems differ, predominately, in the difference in values of ΔG°_{NAC}. We describe here a QM/MM investigation of the *E. coli* chorismate mutase reaction employing two-dimensional energy surfaces to provide additional information concerning the roles of NAC formation and transition state stabilization.

METHODS

The QM/MM procedure that was employed is provided in CHARMM (v31b1). The ligand at the active site (NAC in the ground state and TS) is handled by quantum mechanics (QM = SCCDFTB) calculations, and the enzyme motions are handled by molecular dynamics (*11*−*13*). The initial structure was built from the X-ray structure of the *E. coli* enzyme with the TS analogue [PDB entry 1ECM (*8*)]. A stochastic boundary condition with a radius of 25 Å was centered at the active site, and those atoms beyond 25 Å were not included in the calculations (shown in Figure 2). Within the stochastic boundary, there are 2149 atoms of proteins, 42 X-ray crystal waters, and 1602 TIP3P model water molecules. A Poisson−Boltzmann (PB) charge-scaling scheme was employed to include the correction of long-range electrostatic interactions in the simulation. Poisson−Boltzmann calculations determine a set of scaling factors, which reduce the partial charges of charged residues in the QM/MM electrostatic potential calculations to prevent artifactual structural change (*14*). Molecular dynamics (MD) simulations with a time step of 0.5 fs include both QM and MM. A set of near-attack conformations (NACs) of the enzyme−substrate

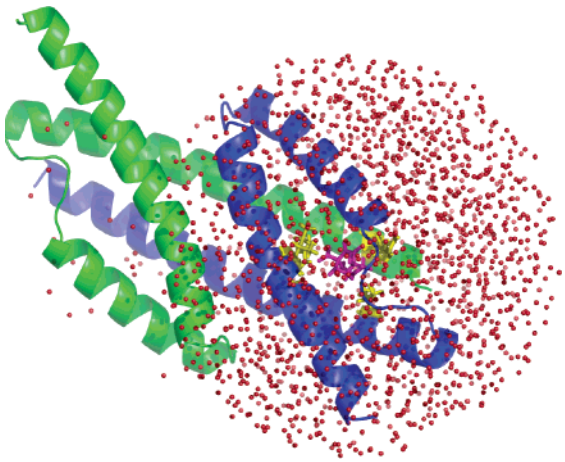

FIGURE 2: View of the *E. coli* chorismate mutase dimer, looking into the active site. The water sphere is represented by red dots. The *E. coli* chorismate mutase dimer is represented by green and purple ribbons. The chorismate is colored magenta, and the residues in the vicinity of chorismate are represented by yellow sticks.

complex (Figure 1) having the appropriate C4−C3−O13−C14 dihedral angle (dih1, 60−70°) and C5−C16 distance (≤3.7 Å) were extracted from the stable trajectory. Their corresponding two-dimensional energy minimization surface was created by a contour plot of the C3−O13 versus C5−C16 distances with 0.1 Å intervals. The positions of the NAC and TS were located, and their structures were determined. Normal-mode analysis was carried out to justify the TS structure obtained from the two-dimensional energy surface. One and only one image frequency was acquired in the frequency analysis of each TS structure, which proves that the structures are on the true saddle point of the energy surface. The C5−C16 and C3−O13 bond lengths for different initial conformations were averaged, as were the energies. The same procedure was employed for chorismate in water, but

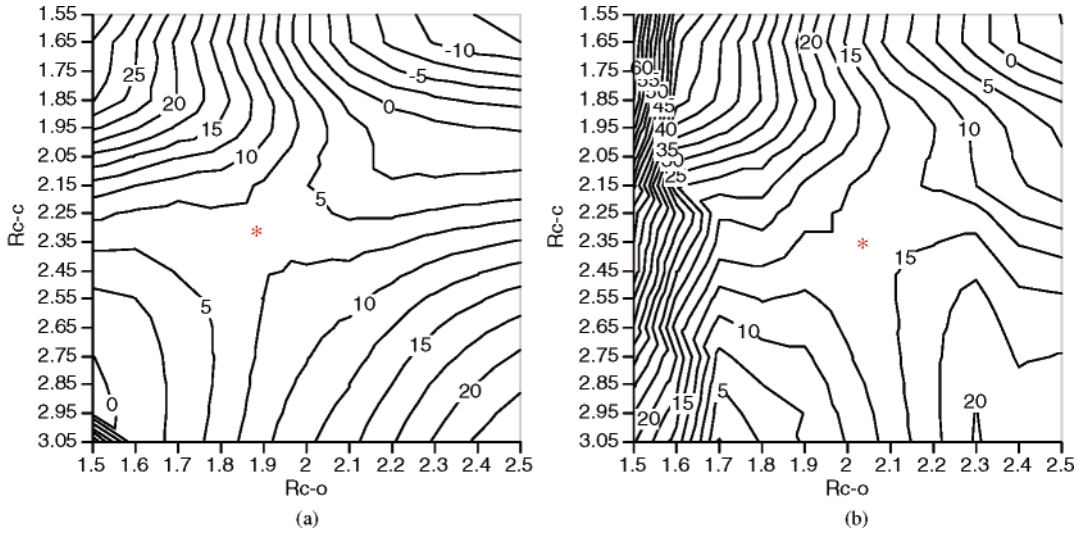

FIGURE 3: Contour plots of the energy profiles in (a) the enzyme and (b) water by using SCCDFTB/MM and two-dimensional reaction coordinates, in which the bond lengths of the forming C−C bond (C5−C16 shown in Figure 1) and the breaking C−O bond (C3−O13 shown in Figure 1) have been used as the reaction coordinates. The positions of the TS are marked with red asterisks. The *y*-axis (Rc-c) of the energy profile in water is plotted with the same scale as that in the enzyme for purposes of comparison, although Rc-c starts from 4.15 Å in water.

required the C5−C16 distance (≤3.7 Å) to be constrained due to the rarity of NAC formation in water. To obtain the electrostatic potential charge of chorismate at the TS, NAC, and ground state in the enzyme, water, and gas phase, the electrostatic potential was calculated at the B3LYP/6-31+G-(d,p) level using the Merz−Singh−Kollman scheme (*15*) implemented in Gaussian 98 (*16*). The restrained electrostatic potential (RESP) method (*17*) was used to fit the electrostatic potential using an atom-centered point charge model.

RESULTS AND DISCUSSION

Energy Profiles and TS Structures. Our results using SCCDFTB/MM show that the average C5−C16 and C3−O13 bond lengths of the TS in the enzyme are 2.32 and 1.90 Å, in water are 2.52 and 2.06 Å, and in the gas phase are 2.55 and 2.00 Å, respectively. These results are in good agreement with the TS structure obtained by Marti et al. (*18*). Bond breaking and making in the TS are concerted regardless of the surrounding milieu or lack thereof. This is a requirement for a pericyclic reaction (*19*, *20*). Results obtained with AM1/MM and SCCDFTB/MM have been compared using exactly the same initial structure, reaction coordinate, and intervals. The ratios of the C3−O13 distance versus the C5−C16 distance in the TS structures in the enzyme, determined by AM1/MM (2.05/1.90 = 1.08) and SCCDFTB/MM (2.32/1.90 = 1.22), are comparable when using the two-dimensional energy surface method (shown in Figure 3).

The activation energy for the formation of the TS structures in water and enzyme via two-dimensional SCCDFTB/MM was corrected for the Coulombic interaction energy (*12*) by single-point B3LYP/6-31+G* theory level calculation (Table 1). These values are ∼11.3 kcal/mol for the enzymatic reaction and ∼20.3 kcal/mol for the reaction in water, compared to the experimental values of 12.7 and 20.7 kcal/mol, respectively (*21*, *22*). Thus, the transition state has been identified as involving concerted bond breaking and making and by the computed energy of reaction being quite similar to the experimental value.

Table 1: Calculated and Corrected Activation Energies (kilocalories per mole) in Enzyme and Water Environments

		enzyme	water	$\Delta\Delta E$
SCCDFTB/MM	ΔE^*	6.1	18.0	11.9
	ΔE°_{NAC}	0.6	11.0	10.4
	ΔE_{TS}	5.5	7.0	1.5
			$\Delta\Delta E^\circ_{NAC}/\Delta\Delta E^* = 87.4\%$	
B3LYP/6-31+G*	ΔE^*	11.3	20.3	9.0
correction	ΔE°_{NAC}	0.3	8.85	8.5
	ΔE_{TS}	11.0	11.4	0.4
			$\Delta\Delta E^\circ_{NAC}/\Delta\Delta E^* = 94.4\%$	
experimental[a]	ΔH^*	12.7	20.7	8.0

[a] The values are taken from refs *21* and *22*. The activation energy with correction by using the equation $\Delta E_{correction} = \Delta E_{SCCDFTB/MM} + (\Delta E^{QM}_{B3LYP/6-31+G^*} - \Delta E^{QM}_{SCCDFTB})$ (*24*).

Stability of the NAC in Catalysis. The differences (eq 1) in the activation energies ($\Delta\Delta E^*$) in water and enzyme are equal to the difference in the energy for NAC formation ($\Delta\Delta E^\circ_{NAC}$) plus the difference in the energy of conversion of the NAC to the TS ($\Delta\Delta E_{TS}$). From the ground state to the NAC, the correction of energy change $\Delta\Delta E^\circ_{NAC}$ is ∼0.3 kcal/mol in the enzyme, which is in agreement with Hur's reports of molecular dynamics and thermodynamic integration results of 0.7 kcal/mol (*1*, *5*−*8*). The smaller free energy for NAC formation in the enzyme, compared to that in water, is supported by the observation of the Karplus group (*23*) that reactive conformations in *B. subtilis* chorismate mutase are plentiful but very rare in water. Therefore, the TS stabilization energy (ΔE_{TS}) from the NAC to the TS equals 11.3 − 0.3 = 11.0 kcal/mol in the enzyme. Computations of the energy for chorismate going to prephenate in water were carried out in exactly the manner employed for the enzyme reaction. The energy for NAC formation (ΔE°_{NAC}) in water is ∼8.85 kcal/mol, the TS stabilization energy (ΔE_{TS}) from the NAC to the TS equals 20.3 − 8.85 = 11.4 kcal/mol in water. The difference in the energies of the NAC → TS reaction ($\Delta\Delta E_{TS}$) in enzyme and water equals 11.4 − 11.0 = 0.40 kcal/mol. This is in reasonable agreement with the value of 1.0 kcal/mol determined by the MD thermodynamic integration studies (*1*). Thus, any TS stabilization by

Table 2: Mulliken Charge and ESP Fitting Charge Distribution of Chorismate at the Ground States and Transition States in Enzyme, Water, and Gas Phase Environments[a]

	ground state in the enzyme				transition states					
	Mulliken		ESP charge		Mulliken			ESP charge		
atom	non-NAC	NAC	non-NAC	NAC	enzyme	water	gas phase	enzyme	water	gas phase
C1	−0.15	−0.15	−0.17	−0.15	−0.13	−0.09	−0.17	−0.16	−0.07	−0.18
C2	0.20	0.20	0.03	0.05	0.23	0.22	0.17	0.14	0.23	0.19
C3	0.19	0.19	0.45	0.55	0.09	0.09	0.03	0.08	0.34	0.04
C4	−0.16	−0.16	−0.47	−0.47	−0.16	−0.13	−0.14	−0.46	−0.45	−0.32
C5	−0.04	−0.04	−0.10	−0.10	0.03	−0.01	0.00	0.10	0.10	0.13
C6	−0.09	−0.08	0.01	−0.02	−0.10	−0.11	−0.09	−0.13	−0.20	−0.22
O13	−0.42	−0.41	−0.55	−0.57	−0.48	−0.49	−0.47	−0.46	−0.51	−0.50
C14	0.17	0.16	0.28	0.30	0.21	0.26	0.24	0.11	0.04	0.12
C16	−0.27	−0.27	−0.59	−0.63	−0.26	−0.28	−0.35	−0.44	−0.28	−0.47

[a] The Mulliken charge was determined with the SCCDFTB/MM method, and the ESP charge was fitted with restrained electrostatic potential method and Merz−Singh−Kollman scheme in Gaussian.

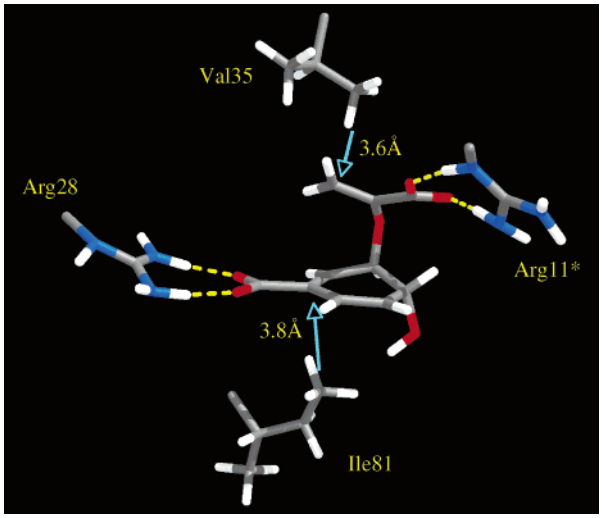

FIGURE 4: Chorismate NAC at the active site of *E. coli* chorismate mutase. Like interactions of NAC occur in the active sites of *B. subtilis* and *T. thermophilus* chorismate mutase (*15*).

the enzyme is comparable to the TS stabilization in water. In these simulations, we have pointed out that the geometry of the active site does not change significantly on the NAC going to the TS (*5*−*8*). This also has been observed by Lee et al. (*25*). The contribution of the stabilization of the chorismate NAC at the active site as compared to the stabilization in water ($\Delta\Delta E^{\circ}_{NAC}$) provides the enzymatic reaction with a kinetic advantage of 8.5 kcal/mol ($\Delta\Delta E^{*} - \Delta\Delta E_{TS}$). Thus, we determine from our QM/MM and high-level QM (B3LYP/6-31+G*) correction calculations that 94% of the efficiency of the enzymatic reaction is due to the stabilization of NAC species. Calculations involving MD thermodynamic integration show that 90% of the enzyme efficiency is derived from the NAC stabilization (*1*, *5*−*8*).

A common catalytic site is present in the various chorismate enzymes. Some major features are shown in Figure 4. The two carboxylates of chorismate form bidentate electrostatic bonds with a pair of arginines which are specifically oriented to hold the substrate in a diaxial conformation that places C5 and C16 adjacent (≤3.7 Å) to each other at angles ($\theta_1 \leq 28.2°$ and $\theta_2 \leq 38.2°$) allowing for appropriate electron orbital overlap for reaction. The substrate is held in the active site as the NAC. The practices (*26*, *27*) of identifying the chorismate NAC by only the distance separating C5 and C16, while ignoring the angles of approach, are tantamount to ignoring the requirement of orbital overlap for the pericyclic reaction. Both C16 and C5 have adjacent hydrophobic amino acid side chains within van der Waals distance. These two amino acids serve as "book ends" to prevent a sideways motion of the C16 and C5 reactants drifting away from each other. The involved arginines in the *E. coli* (*4*, *8*, *9*), *B. subtilis* (*28*), and *Thermus thermophilus* (*10*, *29*) enzymes are R28 and R11*, R7 and R63*, and R6 and R63*, respectively [one arginine comes from the subunit which binds chorismate, and the other arginine (denoted with an asterisk) comes from the adjacent subunit]. The hydrophobic substituents are V35 and I81, L115 and F57, and L114 and F57, respectively. From Hur's previous results (*5*, *7*), it has been shown (*E. coli*) that the distance from C5 to C16 and the distance from Val35 to C16 have no correlation between each other; that is to say, Val35 just acts like a book end and exerts no pushing force on the chorismate. The same phenomenon is also observed in Ile81. Val35 and Ile81 act as a vessel to hold the chorismate.

TS Stability in Catalysis. Our calculations are shown in Table 2. Both Mulliken and ESP charge distribution show that C3 and C5 are almost neutral in the NAC and TS as might be expected in this pericyclic reaction. For the charge on C16, Mulliken charge distributions manifest no significant change from the NAC (−0.27) to the TS (−0.26). However, ESP charge calculation shows that the negative charge decreases from −0.63 (NAC) to −0.44 (TS). A similar phenomenon has also been observed from ESP calculations of O13, which indicates more negative charge in the NAC (−0.57) than in the TS (−0.46). These combined results suggest that the enzyme-bound TS does not have a greater negative charge distribution than the enzyme-bound NAC, and one should not expect larger enzyme electrostatic interactions with the TS than with the NAC. However, examination of the Mulliken partial charge for O13 in E·NAC (−0.41) and E·TS (−0.48) complexes suggests the TS has a marginally greater negative charge than the NAC. The charges of O13 of the TS in water, enzyme, and gas phase are much the same (−0.48, −0.49, and −0.47 for Mulliken charge distribution and −0.46, −0.51, and −0.50 for ESP charge distribution, respectively). Thus, a significant electrostatic stabilization of a developing charge on O13 by a

[2] The use of simple reaction coordinate (difference between the C5−C16 and C3−O13 distances) in previous QM/MM studies (*30*) has provided structures and energies which are not satisfactory.

positive charge at the catalytic site is ruled out. Indeed, the electrostatic interaction in the enzyme should be no more important than the stabilization by a neutral but polar water molecule. This also has been proven by W. W. Cleland's studies of kinetic isotope effects at O13 (*19*). When one goes from the NAC to the TS, the charges of atoms involved in the pericyclic reaction (C3−C5, O13, C14, and C16) do not change much as shown in Table 2. Throughout the chorismate → prephenate *E. coli* reaction O13 is hydrogen bonded to the NH_3^+ group of Lys39. The distances between O13 and the NH_3^+ group of Lys39 in the ground state, NAC, and TS are 2.79, 2.79, and 2.74 Å, respectively. In the NAC and TS, the difference in partial charges (0.07) of O13 and the difference in the distance between O13 and the NH_3^+ group of Lys39 (0.05 Å) speak only for a weak electrostatic stabilization of the TS. The same may be stated for the interaction of Arg90 and O13 in the *B. subtilis* enzyme reaction.

CONCLUSION

Both (a) the combination of molecular dynamics and thermodynamic integrations (*1*, *5*−*7*) and (b) QM/MM and analysis with two-dimensional reaction coordinates[2] have now been used in the study of the mechanism of the chorismate → prephenate reaction. By method (a), the free energy for NAC formation and the free energy of the NAC → TS reaction have been calculated by knowing the experimental value of the reaction activation free energy (ΔG^*). By method (b), the energies of NAC formation (ΔE°_{NAC}) and the energy of the NAC → TS reaction (ΔE_{TS}) are determined directly, as are the TS structures and the NAC and TS atomic charge distributions. The comparable results from methods (a) and (b) are in remarkable agreement. The near identity of TS structures and their charge distributions in the gas phase, in water, and in the enzyme do not support significant electrostatic stabilization of the TS. Also, the charge distributions of the NAC and TS in the enzymatic reaction differ very little and can account for only 10% of the efficiency of the enzymatic reaction. The efficiency of the enzymatic reaction involves a much smaller value of the standard energy for NAC formation (ΔE°_{NAC}) in the enzymes as compared to water.

ACKNOWLEDGMENT

We express appreciation to Dr. Sun Hur and Professor W. Wallace Cleland for helpful discussions.

REFERENCES

1. Bruice, T. C. (2002) A view at the millennium: The efficiency of enzymatic catalysis, *Acc. Chem. Res. 35*, 139−148.
2. Guilford, W. J., Copley, S. D., and Knowles, J. R. (1987) On the mechanism of chorismate mutase reaction, *J. Am. Chem. Soc. 109*, 5013−5019.
3. Copley, S. D., and Knowles, J. R. (1987) The conformational equilibrium of chorismate in solution: Implication for the mechanism of the nonenzymatic and the enzyme-catalyzed rearrangement of chorismate to prephenate, *J. Am. Chem. Soc. 109*, 5008−5013.
4. Bruice, T. C., and Benkovic, S. J. (2000) Chemical basis for enzyme catalysis, *Biochemistry 39*, 6267−6274.
5. Hur, S., and Bruice, T. C. (2002) The mechanism of catalysis of the chorismate to prephenate reaction by the *Escherichia coli* mutase enzyme, *Proc. Natl. Acad. Sci. U.S.A. 99*, 1176−1181.
6. Hur, S., and Bruice, T. C. (2003) Comparison of formation of reactive conformers (NACs) for the Claisen rearrangement of chorismate to prephenate in water and in the *E. coli* mutase: The efficiency of the enzyme catalysis, *J. Am. Chem. Soc. 125*, 5964.
7. Hur, S., and Bruice, T. C. (2003) The near attack conformation approach to the study of the chorismate to prephenate reaction, *Proc. Natl. Acad. Sci. U.S.A. 100*, 12015−12020.
8. Lee, A. Y., Karplus, P. A., Ganem, B., and Clardy, J. (1995) Atomic-structure of the buried catalytic pocket of *Escherichia coli* chorismate mutase, *J. Am. Chem. Soc. 117*, 3627.
9. Ganem, B. (1996) The mechanism of the Claisen rearrangement: Déjà vu all over again, *Angew. Chem., Int. Ed. 35*, 936−945.
10. Helmstaedt, K., Heinrich, G., Merkl, R., and Braus, G. H. (2004) Chorismate mutase of *Thermus thermophilus* is a monofunctional AroH class enzyme inhibited by tyrosine, *Arch. Microbiol. 181*, 195−203.
11. Brooks, B. R., Bruccoleri, R. E., Olafson, B. D., States, D. J., Swaminathan, S., and Karplus, M. (1983) CHARMM: A program for macromolecular energy, minimization and dynamics calculations, *J. Comput. Chem. 4*, 187.
12. Elstner, M., Porezag, D., Jungnickel, G., Elsner, J., Haugk, M., Fraucnhcim, T., Suhai, S., and Seifert, G. (1998) Self-consistent-charge density-functional tight-binding method for simulation of complex materials properties, *Phys. Rev. B 58*, 7260−7268.
13. Cui, Q., Elsstner, M., Kaxias, E., Frauenheim, T., and Karplus, M. (2001) A QM/MM implementation of the self-consistent charge density functional tight binding (SCC-DFTB) method, *J. Phys. Chem. B 105*, 569−585.
14. Simonson, T., Archontis, G., and Karplus, M. (1997) Continuum treatment of long-range interactions in free energy calculations. Application to protein−ligand binding, *J. Phys. Chem. B 101*, 8349.
15. Besler, B. H., Merz, K. M., and Kollman, P. A. (1990) Atomic charges derived from semipirical methods, *J. Comput. Chem. 11*, 431.
16. Frisch, M. J., Trucks, G. W., Schlegel, H. B., Scuseria, G. E., Robb, M. A., Cheeseman, J. R., Zakrzewski, V. G., Montgomery, J. A., Stratmann, R. E., Burant, J. C., Dapprich, S., Millam, J. M., Daniels, A. D., Kudin, K. N., Strain, M. C., Farkas, O., Tomasi, J., Barone, V., Cossi, M., Cammi, R., Mennucci, B., Pomelli, C., Adamo, C., Clifford, S., Ochterski, J., Petersson, G. A., Ayala, P. Y., Cui, Q., Morokuma, K., Malick, D. K., Rabuck, A. D., Raghavachari, K., Foresman, J. B., Cioslowski, J., Ortiz, J. V., Stefanov, B. B., Liu, G., Liashenko, A., Piskorz, P., Komaromi, I., Gomperts, R., Martin, R. L., Fox, D. J., Keith, T., Al-Laham, M. A., Peng, C. Y., Nanayakkara, A., Gonzalez, C., Challacombe, M., Gill, P. M. W., Johnson, B. G., Chen, W., Wong, M. W., Andres, J. L., Head-Gordon, M., Replogle E. S., and Pople, J. A. (1998) *Gaussian 98*, Gaussian Inc., Pittsburgh, PA.
17. Bayly, C. I., Cieplak, P., and Cornell, W. D. (1993) A well-behaved electrostatic potential based method using charge restrained for deriving atomic charges: The RESP model, *J. Phys. Chem. 97*, 10269.
18. Marti, S., Andres, J., Moliner, V., Silla, E., Tunon, I., Vertran, J., and Filed, M. J. (2001) A hybrid potential reaction path and free energy study of chorismate mutase reactions, *J. Am. Chem. Soc. 123*, 1709−1712
19. Gustin, D. J., Mattei, P., Kast, P., Wiest, O., Lee, L., Cleland, W. W., and Hilvert, D. (1999) Heavy atom isotope effects reveal a highly polarized transition state for chorismate mutase, *J. Am. Chem. Soc. 121*, 1756−1757.
20. Cleland, W. W. (2005) Personal communication.
21. Lyne, P. D., Mulholland, A. J., and Richards, W. G. (1995) Insights into chorismate mutase catalysis from a combined QM/MM simulation of the enzyme reaction, *J. Am. Chem. Soc. 117*, 11345−11350.
22. Andrews, P. R., Smith, D., and Young, I. G. (1973) Transition-state stabilization and enzymatic catalysis. Kinetic and molecular orbital studies of the rearrangement of chorismate to prephenate, *Biochemistry 12*, 3492−3498.
23. Guo, H., Cui, Q., Lipscomb, W. N., and Karplus, M. (2001) Substrate conformational transitions in the active site of chorismate mutase: Their role in the catalytic mechanism, *Proc. Natl. Acad. Sci. U.S.A. 98*, 9032−9037.
24. Schmidt, M. W., Baldridge, K. K., Boatz, J. A., Elbert, S. T., Gordon, M. S., Jensen, J. H., Koseki, S., Matsunaga, N., Nguyen,

K. A., Su, S.-J., and Montgomery, J. A. (1993) General atomic and molecular electronic-structure system, *J. Comput. Chem. 14*, 1347.
25. Lee, Y. S., Worthington, S. W., Krauss, M., and Brooks, B. R. (2002) Reaction mechanism of chorismate mutase studied by the combined potentials of quantum mechanics and molecular mechanics, *J. Phys. Chem. B 106*, 12059−12065.
26. Repasky, M. P., Guimaraes, C. R. W., Chandrasekhar, J., Tirado-Rives, J., and Jorgensen, W. L. (2003) Investigation of solvent effects for the Claisen rearrangement of chorismate to prephenate: Mechanistic interpretation via near attack conformations, *J. Am. Chem. Soc. 125*, 6663−6672.
27. Guimaraes, C. R. W., Repasky, M. P., Chandrasekhar, J., Tirado-Rives, J., and Jorgensen, W. L. (2003) Contributions of conformational compression and preferential transition state stabilization to the rate enhancement by chorismate mutase, *J. Am. Chem. Soc. 125*, 6892−6899.
28. Mattei, P., Kast, P., and Hivlert, D. (1999) *Bacillus subtilis* chorismate mutase is partially diffusion-controlled, *Eur. J. Biochem. 261*, 25−32.
29. Zhang, X. H., and Bruice, T. C. (2005) Research in progress.
30. Ranaghan, K. E., Ridder, L., Szefczyk, B., Hermann, J. C., and Mulholland, A. J. (2004) Transition state stabilization and substrate strain in enzyme catalysis: *Ab initio* QM/MM modelling of the chorismate mutase reaction, *Org. Biomol. Chem. 2*, 968−980.

BI050886P